View metadata, citation and similar papers at core.ac.uk
brought to you by CORE
provided by Directory of Open Access Journals

Journal of Engineering Science and Technology
Vol. 8, No. 3 (2013) 326 - 343
© School of Engineering, Taylor's University

MODELING OF TRANSIENT HEAT TRANSFER IN FOAMED CONCRETE SLAB

MD AZREE OTHUMAN MYDIN

School of Housing, Building and Planning, Universiti Sains Malaysia, 11800, Penang, Malaysia
E-mail: azree@usm.my

Abstract

This paper reports the basis of one-dimensional Finite Difference method to obtain thermal properties of foamed concrete in order to solve transient heat conduction problems in multi-layer panels. In addition, this paper also incorporates the implementation of the method and the validation of thermal properties model of foamed concrete. A one-dimensional finite difference heat conduction programme has been developed to envisage the temperature development through the thickness of the foamed concrete slab, based on an initial estimate of the thermal conductivity-temperature relationship as a function of porosity and radiation within the voids. The accuracy of the model was evaluated by comparing predicted and experimental temperature profiles obtained from small scale heat transfer test on foamed concrete slabs, so that the temperature history of the specimen calculated by the programme closely matches those recorded during the experiment. Using the thermal properties of foamed concrete, the validated heat transfer program predicts foamed concrete temperatures in close agreement with experimental results obtained from a number of high temperature tests. The proposed numerical and thermal properties are simple yet efficient and can be utilised to aid manufacturers to develop their products without having to conduct numerous large-scale fire tests.

Keywords: Foamed concrete, Thermal analysis, Thermal properties, Heat transfer, Elevated temperatures, Thermal conductivity.

1. Introduction

Foamed concrete is a material having a minimum of 20 per cent by volume of mechanically entrained foam in the mortar slurry. It is produced by entrapping numerous small voids of air in cement paste. Mechanical foaming can take place in two principal ways; by pre-foaming a suitable foaming agent with water and then combining the foam with the paste or by adding a quantity of foaming agent to

Nomenclatures

c	Specific heat of material, J/kg°C
c_p	Overall specific heat capacity, J/kg°C
c_{pi}	Component specific heat, J/kg°C
d	Specimen thickness, mm
e	Effective emissivity
e_w	Dehydration water content, %
F_i	Weight fraction of each component
f	Modification factor accounting for water movement
h	Convection heat transfer coefficient, $W/m^2.K$
k^*	Effective thermal conductivity, W/m.K
L	Thickness of the panel, mm
T	Temperature, ^oC
T_0	Initial temperature, ^oC
T_∞	Ambient temperature, °C
t	Time, s
x, y, z	Cartesian coordinates

Greek Symbols

Δc	Average additional specific heat, J/kg°C
ΔT	Temperature difference,°C
σ	Stefan-Boltzmann constant, W/m^2K^4
ρ	Density, kg/m^3
Φ	Geometric view factor
ε	Porosity

the slurry and whisking the mixture into a stable mass with the required density. The most frequently used foam concentrates are based on hydrolyzed protein or synthetic foaming agents. They are formulated to produce air voids that are stable and capable to resist the physical and chemical forces imposed during mixing, placing and hardening. Foam concrete is very sensitive to water demand compared to normal concrete. If too little water is added to the mixture, the water will not be sufficient for initial reaction of the cement and the cement will extract water from the foam, causing speedy disintegration of the foam. If too much water is added in the mixture, segregation will happen causing dissimilarity in density.

Foamed concrete is a complex material, which acts in correctly complex way. Its properties deviate with age, temperature and humidity. Furthermore, at near the beginning ages, heat is generated which may result in substantial temperature increase. It therefore becomes difficult to anticipate its behavior with any real precision, even under controlled conditions, and the use of published information must be attentively qualified unless the conditions of application are close to those under which the information was acquired.

When foamed concrete been exposed to elevated temperatures, the free water in the pores and some chemically bounded water in the cement paste are released, consuming a large amount of energy. A few authors have described, as follows, the reactions that occur in cement based material like foamed concrete at elevated temperatures. Vaporization of the free water takes place at around 100°C [1]. It is normally considered that the evaporable water is entirely eradicated at the

temperature of 120°C. Subsequently between the temperatures of 180 to 300°C, loss of the chemically bound water occurs through decomposition of the C-S-H and carboaluminate hydrates [2]. The elevated temperatures in the range of 400 to 600°C may then stimulate a series of reactions in the hardened foamed concrete paste. These reactions instigate with the inclusive dehydration of the pore system and then followed by decomposition of the hydration products and the destruction of C-S-H gels [3]. The alteration of calcium hydroxide into lime and water vapour during heating may guide to serious damage due to lime expansion [4].

Given that foamed concrete is a porous material, the effective thermal conductivity will be affected by the air voids inside the cement paste. Inside each air void, heat conduction will dominate at comparatively low temperatures. Nevertheless, at elevated temperatures, radiation will play a much more significant role because the radiation coefficient is related to temperature raised to power three. The effective thermal conductivity of foamed concrete at elevated temperatures depends not only on the thermal conductivities of the cement and the air, but also radiation effect inside the air voids.

For that reason, to assess fire resistance of foamed concrete, it is indispensable to study temperature history of this material in fire conditions. Whilst similar principles of heat transfer govern the temperature development throughout material, different analytical or numerical methods may be practical to acquire the solution. In order to attain thermal properties of foamed concrete, a one-dimensional heat transfer model is adequate and Finite Difference Method (FDM) emerges to be the simplest method to be executed.

This paper presents the development of one-dimensional finite difference model which can be used to solve transient heat conduction problems in multi-layer panels. Convection and radiation boundary conditions on both fire exposed side and unexposed side of the material are also considered. In addition, thermal property models and their validation using the experimental results will also be presented. The thermal parameters considered are density, specific heat and thermal conductivity.

2. Numerical analysis method

The transient heat transfer through foamed concrete is modelled using one-dimensional Finite Difference formulation. A computer program to model the transient heat transfer through foamed concrete has been developed and implemented in the familiar environment of Microsoft Excel using VBA based on one-dimensional Finite Difference formulations.

The modelling procedure has been systematically validated by comparisons with a number of analytical solutions and simulation results using ABAQUS/Standard. The next section will describe the basis of the modelling method which includes the development of one-dimensional Finite Difference formulation which can be used to solve transient heat conduction problems for porous material.

2.1. Fundamental formulation

Assuming a homogenous and isotropic material, the general three-dimensional transient heat-conduction equation (based on Fourier's law of conduction) in Cartesian coordinates is [5]:

$$\rho c \frac{\partial T}{\partial t} = \frac{\partial}{\partial x}\left(k \frac{\partial T}{\partial x}\right) + \frac{\partial}{\partial y}\left(k \frac{\partial T}{\partial y}\right) + \frac{\partial}{\partial z}\left(k \frac{\partial T}{\partial z}\right) \quad (1)$$

The right hand side of Eq. (1) stand for the net heat conduction in a solid material, whereas the left hand side represents the accumulated internal energy.

Calculation of heat flow in solids is based on the solution of this differential equation. Due to complexity of many geometric shapes and boundary conditions of practical interest, analytical solutions to Eq. (1) are not always possible. Finite Difference Method is a relatively simple technique which can provide approximate numerical solutions to many practical cases. FDM replaces derivative expressions in Eq. (1) with approximately equivalent partial difference quotients. Two approaches can be taken to transform the partial differential equation into finite difference equation; mathematical replacement approach and physical heat balance approach.

The two techniques often result in the same finite difference equations. However, the heat balance technique might suit better to irregular boundaries with convective heat loss [6] and therefore is adopted in this study. In this approach one includes a control volume around each grid point and locally applies direct approximations to the energy balance principles to this volume. In other words, the method considers the heat flow into and out of the cell for a particular time-step and determines the temperature change of the cell based on its mass and specific heat.

The resultant finite difference equations can be either explicit or implicit. In the implicit approach a set of simultaneous equations has to be solved at each step in time. Although the solution process is relatively complex, it allows for the use of larger time intervals. In the explicit approach, on the other hand, the temperature of a volume cell at a time step is computed directly based on the temperatures of the adjacent cells in the last time step, leading to a very simple scheme of computation [6]. However, the time interval required can sometimes be inconveniently small.

2.2. Explicit finite difference formulation for a multi-layer panel

Given the simplicity and effectiveness the explicit approach in finite difference method provides, it was found suitable for the purpose of this study. Although time intervals required in this method are small, it does not cause any further complications to the computations, since small time steps are already necessary in fire resistance analysis due to rapid changes of temperature in fire conditions.

If the thickness of the foamed concrete panel is small in comparison to the other dimensions, the problem will reduce to a one dimensional heat transfer analysis, i.e., the heat flow is perpendicular to the face except near the edges. Hence, the governing Eq. (1) with no heat generation reduces to:

$$\rho c \frac{\partial T(x,t)}{\partial t} = \frac{\partial}{\partial x}\left(k(T) \frac{\partial T(x,t)}{\partial x}\right) \quad (2)$$

where $0 \leq x \leq L$, for $t > 0$, L is the thickness of the panel.

Assuming a homogeneous material and choosing the explicit method, the temperature of a volume cell (Figs. 1 and 2) at a time step is computed directly

based on the temperatures of the adjacent cells in the last time step which leads to a very straightforward scheme of computation [7]:

(i) For a typical node *m* within the material (Fig. 1):

$$T'_m = F_0[\frac{2(k_{m-1,m}T_{m-1} + k_{m+1,m}T_{m+1})}{k_{m-1,m} + k_{m+1,m}} + T_m(\frac{1}{F_0} - 2)] \quad (3)$$

where F_0 is defined as:

$$F_0 = \frac{(k_{m-1,m} + k_{m+1,m})\Delta t}{2\rho c(\Delta x)^2} \quad (4)$$

T'_m is the temperature of *m* in the subsequent time step and $k_{i,j}$ is the thermal conductivity at the average temperature of cells *i* and *j*:

$$k_{i,j} = k(\frac{T_i + T_j}{2}) \quad (5)$$

Numerical stability under the explicit scheme requires:

$$\Delta t \le \frac{\rho c(\Delta x)^2}{(k_{m-1,m} + k_{m+1,m})} \quad (6)$$

(ii) For a boundary node, when subjected to convective and radiative boundary conditions (Fig. 2):

$$T_1^{'} = 2F_0[T_2 + \frac{h\Delta x}{k_1}T_\infty + (\frac{1}{2F_0} - 1 - \frac{h\Delta x}{k_1})T_1) + \phi e\sigma[(T_\infty + 273)^4 - (T_1 + 273)^4]\frac{2\Delta t}{\rho c\Delta x} \quad (7)$$

where F_0 is $F_0 = \frac{k_1\Delta t}{\rho c(\Delta x)^2}$

Numerical stability limits the time step to:

$$\Delta t \le \frac{0.5\rho c(\Delta x)^2}{k_1}[1 + \frac{h\Delta x}{k_1} + \frac{\phi E\sigma\Delta x}{k_1} \cdot \frac{(T_1 + 273)^4}{T_1}]^{-1} \quad (8)$$

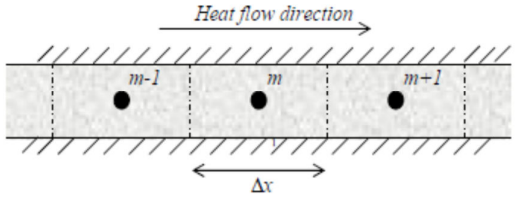

Fig. 1. Finite Difference Discretization for Node *m* within the Material.

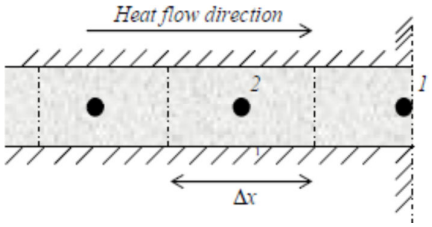

Fig. 2. Finite Difference Discretization for Boundary Node.

2.3. Initial and boundary conditions

Foamed concrete panel is understood to have a uniform initial temperature equal to the ambient temperature. On the unexposed boundary, the convective heat transfer coefficient (h) is assumed to be constant and the value is taken as 10 W/m^{2}K [8]. The emissivity of the surface depends on the material. For concrete, the surface emissivity will be taken as 0.92 [9]. The exposed boundary conditions are the recorded temperatures on the exposed surface of fire test specimens.

3. Validation of the Heat Conduction Model

Section 2 has comprehensively extracted the Finite Difference formulations to model the one-dimensional transient heat transfer through foamed concrete and its initial and boundary conditions. It is important to verify the accuracy of this model through comparison with the available analytical and numerical solutions. To accomplish this validation, three different approaches have been taken as follows:

1) Verification of the conductive heat transfer simulation through a panel (case 1)
2) Verification of the convective heat transfer at boundaries of a panel (case 2)
3) Verification of the conductive heat transfer simulation with temperature-to dependent material properties (case 3).

For case 1 and 2, analytical solutions are presented with constant material properties of foamed concrete. Nevertheless no analytical solution is established when thermal properties of the material change with temperature (case 3). Therefore, numerical simulation results using the generic commercial finite element package, ABAQUS, are employed to corroborate the Finite Difference formulations.

3.1. Conduction heat transfer with constant material properties

Consider a one-dimensional heat transfer through foamed concrete slab with thickness l and constant thermal conductivity, k. The initial temperature of the panel is uniform and indicated by T_0 (Fig. 3). If both surfaces of the foamed concrete panel are suddenly changed at a temperature of 0°C, temperature development through the thickness of the panel at time t can be calculated as follow [10]:

$$T = \frac{4T_0}{\pi}\sum_{n=0}^{\infty}\frac{1}{2n+1}e^{-\alpha(2n+1)^2\pi^2 t/l^2}\sin\frac{(2n+1)\pi x}{l} \tag{9}$$

where $\alpha = \dfrac{k}{\rho c}$, ρ is the density of the material and c is the specific heat.

Analysis has been carried out for an example of case 1 (Fig. 3) with the material properties indicated in Table 1.

The temperature development of this example is achieved through both the analytical method, Eq. (9) and the Finite Difference method. The results are compared in Figs. 4 and 5. The thickness of the slab is divided into 6 elements and temperatures are calculated for the nodes indicating each element (5 internal nodes and 2 boundary nodes) and the time step of 5 seconds is used for this Finite

Difference method. The infinite series in Eq. (9) has been restricted to only 12 members for calculation purposes. It can be seen in Figs. 4 and 5 that Finite Difference method can offer very accurate results for heat transfer analysis in solids with constant thermal properties regardless of its simple approach.

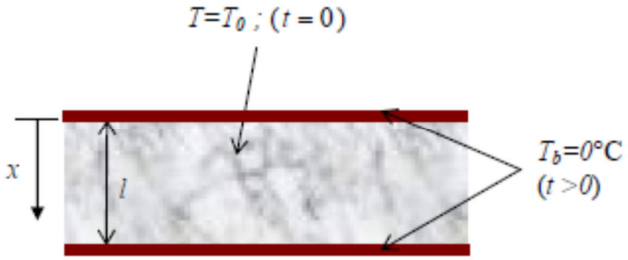

Fig. 3. Foamed Concrete Slab with Thickness *l*, Both Boundaries Kept at Zero Temperature.

Table 1. Material Properties of Foamed to Concrete Analyse Example of Case 1.

LFC properties	Values
Density (ρ)	650 kg/m^3
Thickness of panel (l)	30 mm
Thermal conductivity (k)	0.206 W/mK
Specific heat (c)	1110 J/kg.°C
Initial temperature (T_0)	20°C

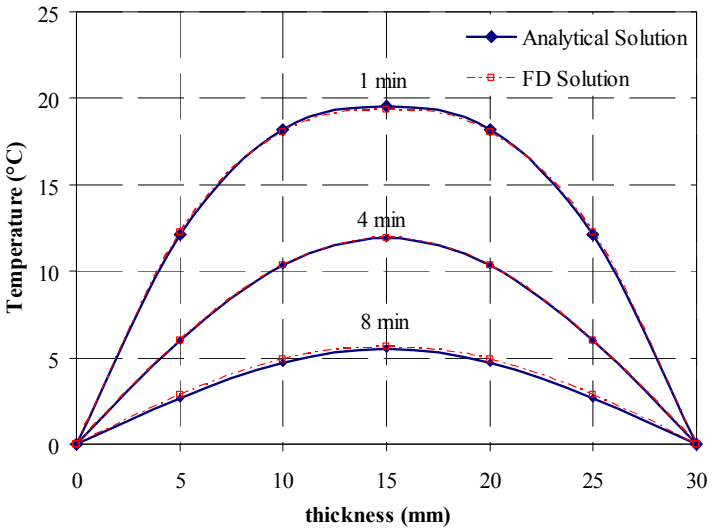

Fig. 4. Temperature Distribution across the Thickness of a 30 mm Slab Example Attained by Analytical Method and Finite Difference Method.

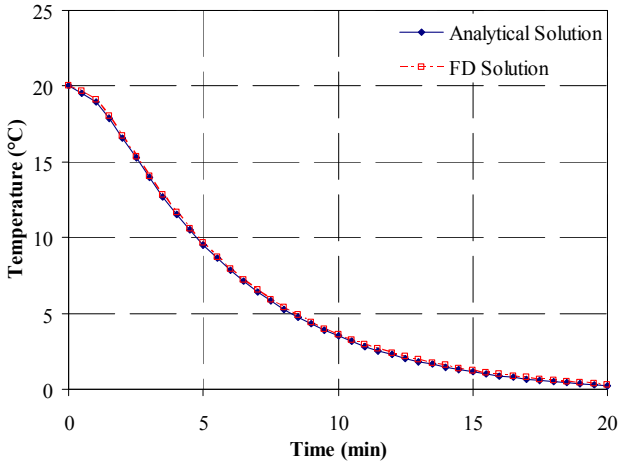

Fig. 5. Temperature Development at the Midpoint of a 30 mm Obtained by Example Slab Analytical Method and Finite Difference Method.

3.2. Convection heat transfer with constant material properties

Verification is also carried out for a problem where convective boundary conditions exist. Consider the one-dimensional heat transfer through a slab with thickness of 2*L* and constant thermal conductivity of *k* shown in Fig. 6.

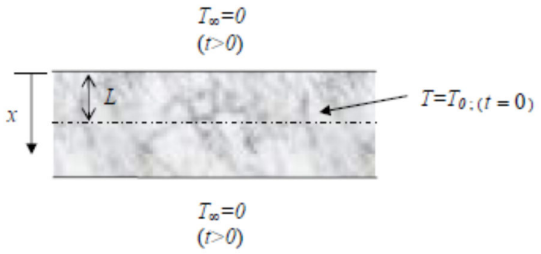

Fig. 6. A Panel with Thickness 2*L*, Suddenly Entered at a Temperature of 0°C.

The initial temperature of the panel is T_0. The slab is suddenly taken to an ambient temperature of T_∞ and the convective heat transfer coefficient at the surfaces of the panel is *h*. If $\theta=T-T_\infty$, temperature development across the thickness of the panel at time *t* can be calculated using the following equation [11]:

$$\frac{\theta}{\theta_0}=2\sum_{n=1}^{\infty}\frac{\sin\lambda_n}{\lambda_n+\sin\lambda_n\cos\lambda_n}\cdot\exp\left(-\lambda_n^2\alpha t/L^2\right)\cdot\cos\left(\lambda_n x/L\right) \tag{10}$$

where $\alpha=\dfrac{k}{\rho c}$ and λ_n are roots of the equation: $\lambda_n\tan\left(\lambda_n\right)=\dfrac{hL}{k}$

Analysis has been carried out for an example of case 2 (Fig. 6) with the material properties indicated in Table 2.

Table 2. Material Properties of Foamed to Concrete Analyse Example of case 2.

LFC properties	Values
Density (ρ)	650 kg/m^3
Thickness of panel (L)	15 mm
Thermal conductivity (k)	0.206 W/mK
Heat transfer coefficient (h)	10 W/m^{2}K
Specific heat (c)	1110 J/kg.°C
Initial temperature (T_0)	20°C
Ambient temperature (T_∞)	0°C

The first 20 roots of λ_n are used in Eq. (10). The time step of 5 seconds is employed in the Finite Difference analysis and the thickness of the panel is divided by 7 nodes. The results are compared in Figs. 7 and 8. Obviously results in Figs. 7 and 8 showed that Finite Difference method is in good agreement with the analytical results.

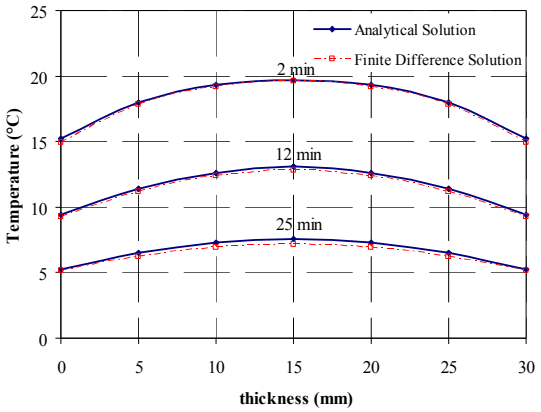

Fig. 7. Temperature Distributions across the Thickness of a 30 mm Example Slab with Convective Boundary Condition by Attained Analytical Method and Finite Difference Method.

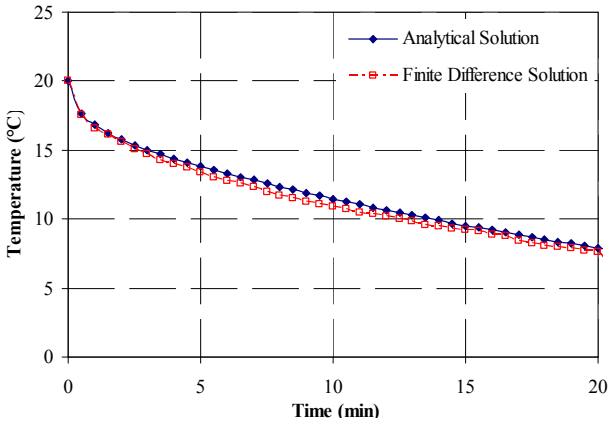

Fig. 8. Temperature Developments at the Surface of a 30 mm Example Slab with Convective Boundary Condition by Attained Analytical Method and Finite Difference Method.

3.3. Heat transfer with temperature-dependent thermal properties

The thermal properties of foamed concrete are temperature-dependant. Since analytical solutions for heat transfer through this material is not available, another numerical method, Finite Element analysis, is employed for validation of Finite Difference analysis. For validation purpose, a 30 mm foamed concrete slab initially at 25°C is considered.

The temperature-dependent thermal properties of the foamed concrete slab are modelled as explained in Section 4, with density of 650 kg/m^3 at ambient temperature. One surface of the slab is exposed to high temperatures and the other side faces the ambient temperature of 25°C. Figure 9 illustrates the temperature curve obtained experimentally on the exposed surface of the slab and compares the temperature predictions of the unexposed side by the proposed Finite Difference analysis and by Finite Element analysis using the common software package, ABAQUS. It should be pointed out the expose surface temperature is represented as a curve because continuous reading was acquired during the testing. The validity of Finite Difference formulations is confirmed yet again. The validation of Finite Difference formulations confirmed that even though explicit Finite Difference method is a fairly simple algorithm, it could still offer very precise results compared to analytical methods or other complicated numerical ones.

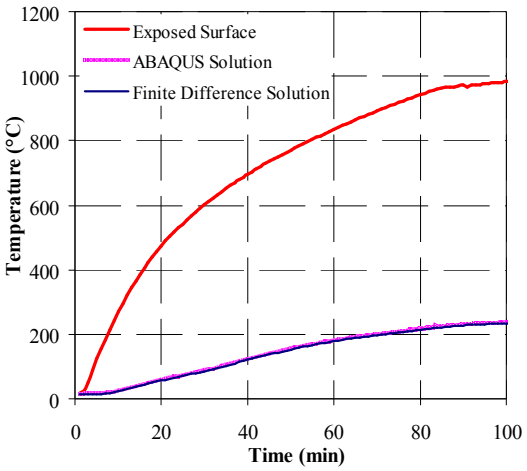

Fig. 9. Temperature Developments on the Unexposed Surface of a 30 mm Foamed Concrete Slab Attained by ABAQUS (Finite Element Analysis) and Finite Difference Method.

4. Material Properties

The proposed numerical method can be used to predict the thermal response of foamed concrete given the appropriate material properties. Foamed concrete is a composite material made from a combination of sand, cement binder and water. After mixing, the cement hydrates and hardens into a stone like material. Theoretically, combined mass and heat transfer should be carried out to obtain temperatures in foamed concrete construction. However, modelling mass transfer (water movement)

is complex. A common approximation is to conduct heat transfer only, but modifying the material thermal properties to reflect the effects of water movement.

In order to utilize the proposed numerical method for heat transfer analysis, data on density, specific heat and thermal conductivity should be provided. This section will only present summary of these data which were based on comprehensive experimental investigation on thermal properties of foamed concrete (density of 650kg/m^3) conducted by the author [8].

4.1. Density

Evaporation of the free and of some of the chemically bound water will cause dehydration in foamed concrete, which will affect all the aforementioned three items of thermal properties. The dehydration process starts as early as 90°C [8]. Figure 10 shows recorded density of foamed concrete at different temperatures, as ratio of the original density for initial density values of 650 kg/m^3.

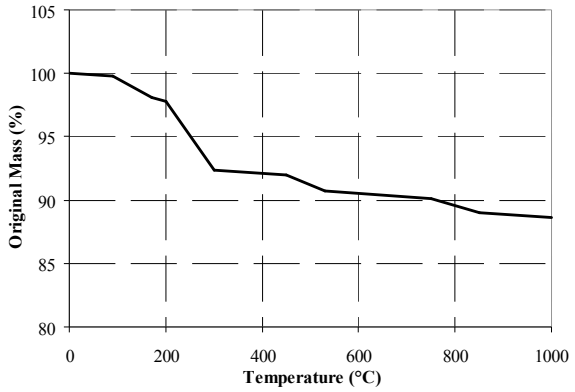

Fig. 10. Relative Mass of Foamed Concrete as a Function of Temperature.

The results presented in Fig. 10 were obtained by weighing specimens. Usually thermo gravimetric analysis (TGA) is performed on very small samples to determine changes in weight in relation to change in temperature. Nevertheless, due to limitation in experimental facility, the weight loss of foamed concrete samples for this study was measured manually after exposure to certain temperature point. In order to determine the weight loss of foamed concrete specimens as a function of temperature, three 100×100 mm × 100 mm LFC cubes of 650 kg/m^3 were heated in the electric kiln. The cubes were kept in each temperature point for 24 hours and their weight loss was recorded. Then the temperature was raised at the rate of 20°C/day. The procedure was continued until a maximum temperature of 1000°C. It should be pointed out that the change in volume with temperature in the calculation of density is not considered.

4.2. Specific heat

The specific heat of foamed concrete may be divided into two parts: the base value corresponding to a mixture of the dry components and the effect of water

evaporation. The temperature-dependent specific heat of foamed concrete experience one peak corresponding to the dehydration reaction of foamed concrete between 90°C to 170°C as shown in Fig. 11. This peak represents the energy consumed to dissociate and evaporate water and include the effect of water movement and recondensation of water in cooler regions of foamed concrete.

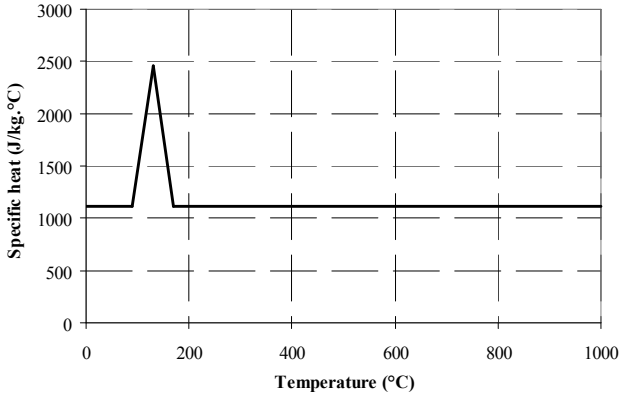

Fig. 11. Specific Heat of Foamed Concrete as a Function of Temperature.

The calculated base value of specific heat at ambient temperature for 650 kg/m^3 density was 1110 J/kg°C [8] and the additional specific heat at the dehydration reaction can be expressed by:

$$\Delta c = \frac{2.26\times10^6}{\Delta T}\times e_w \times f \quad \text{(J/kg°C)} \tag{11}$$

in which the value of 2.26×10^6 J/kg is the latent heat of evaporation of water, Δ_c is the average additional specific heat, e is dehydration water content (percentage by total weight), Δ_T is the magnitude of the temperature interval during which water is evaporated and f is a modification factor accounting for water movement. A value of f =1.4 was used for standard fire conditions. Figure 11 shows the temperature-dependent specific heat of 650 kg/m^3 density [8].

4.3. Thermal conductivity

Since foamed concrete is a porous material, heat transfer through this material is a combination of all three modes: conduction through the solid and convection and radiation through the pores. Therefore the effective thermal conductivity of foamed concrete should include these effects. This effective thermal conductivity can be affected by many factors such as temperature, density, moisture content and porosity of the material. Assuming foamed concrete is made of solid substrate and uniformly distributed spherical pores, the effective thermal conductivity of foamed concrete may be calculated using the following equation [12]:

$$k^* = k_s \frac{k_g \varepsilon^{\frac{2}{3}} + (1-\varepsilon^{\frac{2}{3}})k_s}{k_g(\varepsilon^{\frac{2}{3}} - \varepsilon) + (1-\varepsilon^{\frac{2}{3}} + \varepsilon)k_s} \tag{12}$$

where k^* is the effective thermal conductivity of foamed concrete, k_g is effective thermal conductivity of gas to account for heat transfer in the pores, k_s is the thermal conductivity of the solid and ε is the porosity of the material (the ratio of the volume of void pore to the overall volume).

In this study, the thermal conductivity of solid dried foamed concrete (k_s) is 0.5 W/m.°C and the porosity of 650 kg/m^3 density is 75% [8].

Since the size of the pores is very small (never larger than 5 mm), natural convection in the pores can be neglected [8]. Therefore the effective thermal conductivity of the gas is:

$$k_g = 4.815\times10^{-4}T^{0.717} + \frac{2}{3}\times 4d_e\sigma T^3 \tag{13}$$

where T is absolute temperature and d_e is the effective diameter of the pores. In this study d_e = 0.72 mm for 650 kg/m^3 density [8]. The first term is the gas thermal conductivity without the effect of thermal radiation and the second term represents the effect of radiation within the air pores.

The porosity values of foamed concrete were obtained through the Vacuum Saturation Apparatus [13]. The measurements of foamed concrete porosity were conducted on slices of 68 mm diameter cores cut out from the centre of 100 mm cubes. The specimens were dried at 105°C until constant weight had been attained and were then placed in a desiccator under vacuum for at least 3 hours, after which the desiccator was filled with de-aired, distilled water. The porosity is calculated using the following equation:

$$\varepsilon = \frac{W_{sat} - W_{dry}}{W_{sat} - W_{wat}}\times 100 \tag{14}$$

where ε is the porosity (%), W_{sat} is the weight in air of saturated sample, W_{wat} is the weight in water of saturated sample and W_{dry} is the weight of oven-dried sample.

On the other hand, the specimen preparation for the measurement of the pore size was slightly different then from recommended by ASTM C 457 [14]. ASTM C 457 specified the size and thickness of the specimen and length of travel in the linear traverse method (LTM), based on the size of aggregate. Mixtures from this study, however, do not contain any coarse aggregate but consist of high amounts of air (foam). In order to ensure the stability of the air pore walls during polishing, particularly in weaker specimens (lower density), all the specimens were vacuum-impregnated with slow-setting epoxy. To ensure consistency in results, all the specimens were prepared using similar techniques under the same environmental conditions, as follows.

Foremost, the specimens of 45×45 mm size with a minimum thickness of 15 mm were cut from the centre of two randomly selected 100 mm cubes using a diamond cutter. The face of the specimen was cut perpendicular to the casting direction. Sized specimens were saturated in acetone to stop further hydration reaction before drying at 105 °C. To ensure the stability of the air-pore walls during polishing, the dried and cooled specimens were vacuum impregnated with slow-setting epoxy. The impregnated specimens were polished as per ASTM C 457. After polishing and cleaning, the specimens were dried at room temperature for 1 day. Finally, an effective size 40×40 mm was considered for pore size measurement. The pore size were measured according to ASTM C 457 under a microscope with a magnification

of 60x on two specimens, prepared as per the procedure described previously, for each foamed concrete specimen. Image analysis system consisted of an optical microscope and a computer with image analysis software.

Hence, the effective thermal conductivity-temperature relationship of 650 kg/m^3 density foamed concrete consists of three parts as demonstrated in Fig. 12: (i) Constant thermal conductivity up to 90°C before water evaporation, equal to that at ambient temperature reported by the manufacturer; (ii) Linear reduction of conductivity to 0.14 W/m.°C at 170°C; (iii) Non-linear increase in thermal conductivity based on Eqs. (12) and (13).

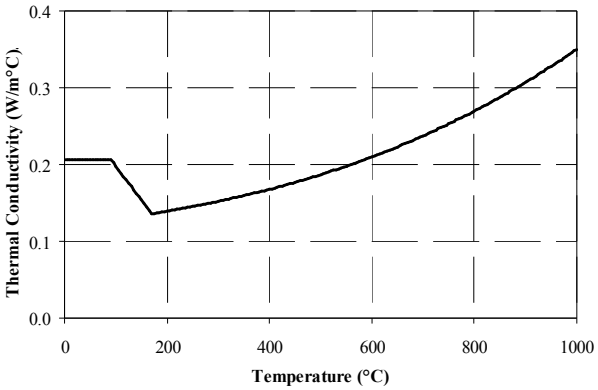

Fig. 12. Effective Thermal Conductivity of Foamed Concrete as a Function of Temperature.

5. Small Scale Heat Transfer Test on Foamed Concrete Slab

A limited number of small-scale experiments have been performed on 650 kg/m^3 density foamed concrete slab. All foamed concrete slab specimens had dimensions of (430×415) mm in plan and 150 mm in thickness. Each specimen was placed horizontally on top of an electric kiln as the source of heat, so that one side of the panel was subjected to kiln temperature and the other side faced up to the room temperature (19-25°C). The heating chamber has an internal diameter of 648 mm and 534 mm height. There was a (280×265) mm opening on the top lid of the kiln, which allowed exposure of the lower side of the panel to elevated temperatures. A 30 mm thick layer of glass wool with the same opening size was laid under the specimen to insulate the contact surface of the top lid. The kiln temperature was increased to about 1200°C.

Type K thermocouples were placed throughout the thickness of the foamed concrete specimen at the centre of the slab to investigate temperature developments through each foamed concrete panel. Five thermocouples were installed: on the exposed side, on the unexposed side and at quarter, half and three-quarter thickness, being 37.5 mm, 75 mm and 112.5 mm from the heated surface. One thermocouple was place inside the kiln, at an approximate distance of 50 mm from the exposed surface of the panel, to record the kiln temperature. Figure 13 shows typical set-up of the experiments.

Fig. 13. Typical Set-up for the Small-scale Fire Tests.

6. Validation of Thermal Property Models

In order to validate the proposed thermal property models for foamed concrete presented in Section 4, thermal property values from these models were used as input material properties in the one-dimensional heat transfer program to predict temperature developments inside the foamed concrete slab test samples presented in Section 2 of this paper. It is acceptable to assume that heat transfer in the test samples is one-dimensional in the thickness direction of the foamed concrete slab [8]. Measured experimental temperatures at all recording locations of the test specimens were compared with numerical analysis results, to provide comprehensive validation of the thermal property models presented in Section 4. Thermal property values (theoretical thermal property model results) are considered and their prediction results compared. As mentioned previously, the exposed surface temperatures are used as input data in the heat transfer analysis to eliminate uncertainty in the thermal boundary condition on the exposed side. Figures 14-17 compare the measured and numerical analysis results for the 650 kg/m^3 density specimens. The results shown in Figs. 14-17 clearly indicate close agreement between prediction and measured results of temperature throughout the thickness of the foamed concrete samples.

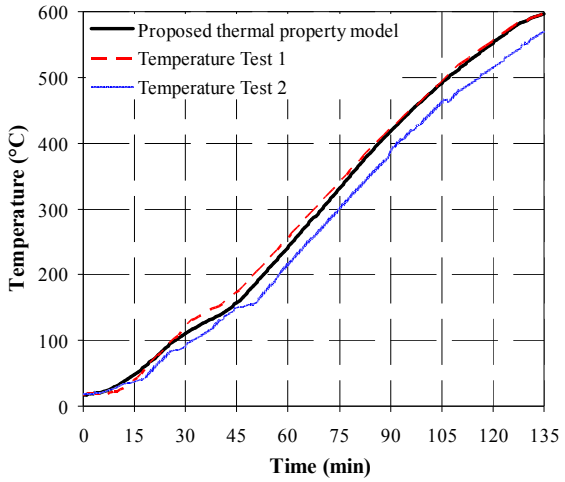

Fig. 14. Comparison between Test Results and Numerical Analysis at 37.5 mm from Exposed Surface.

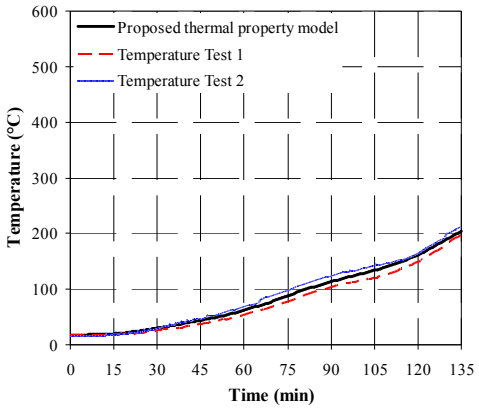

Fig. 15. Comparison between Test Results and Numerical Analysis at 75 mm from Exposed Surface.

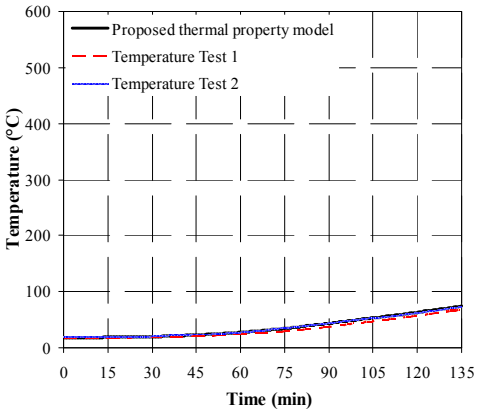

Fig. 16. Comparison between Test Results and Numerical Analysis at 112.5 mm from Exposed Surface.

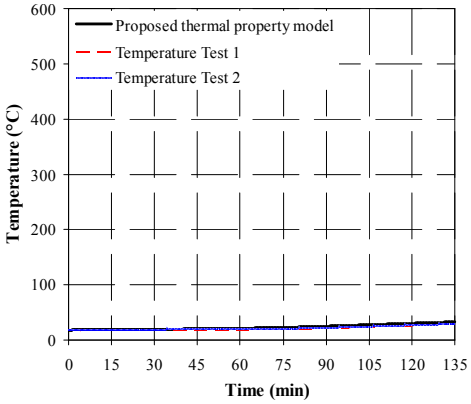

Fig. 17. Comparison between Test Results and Numerical Analysis at UnExposed Surface.

7. Conclusions

This paper has presented the basis of the one-dimensional heat transfer modelling, the implementation of the method and the validation of thermal properties model of foamed concrete slab. The comparison of test results with the numerical heat transfer analysis results using the proposed thermal property models is close, confirming the validity of the thermal conductivity models. Despite simplicity, the aforementioned analytical models for specific heat and thermal conductivity of foamed concrete of different densities give accurate results. The proposed model is straightforward yet proficient and can be exploited to assist manufacturers to develop their products without having to carry out numerous large-scale fire tests in the future.

Acknowledgement

The author would like to thank Universiti Sains Malaysia and Ministry of Higher Education Malaysia for their financial supports under Fundamental Research Grant Scheme (FRGS), No. 203/PPBGN/6711256.

References

1. Noumowe, A. (1995). *Effets des hautes temperatures* (20°*C* - 600°C) *sur le beton. Cas particulier du béton à hautes performances*. Ph.D. Thesis, Institute National des Sciences Appliquees.
2. Khoury, G.A. (1992). Compressive strength of concrete at high temperatures: A reassessment. *Magazine of Concrete Research*, 44(161), 291-309.
3. Rostasy, F.S.; Weiβ, R.; and Wiedemann, G. (1980). Changes of pore structure of cement mortars due to temperature. *Cement and Concrete Research*, 10(2), 157-164.
4. Lin, W.M.; Lin, T.D.; and Powers-Couche, L.J. (1996). Microstructures of fire-damaged concrete. *ACI Material Journal*, 93(3), 199-205.
5. Holman, J.P. (2002). *Heat Transfer*. Ninth Ed., McGraw-Hill, London.
6. Croft, D.R. and Lilley, D.G. (1977). *Heat transfer calculations using finite difference equations*. Applied Science Publishers, London.
7. Wang, H.B. (1995). *Heat transfer analysis of components of construction exposed to fire*. Department of Civil Engineering and Construction, University of Salford, Manchester.
8. Othuman Mydin, M.A.; and Wang, Y.C. (2011). Elevated-temperature thermal properties of lightweight foamed concrete. *Journal of Construction and Building Materials*, 25(2), 705-716.
9. Ozisik, M.N. (1985). *Heat transfer: A basic approach.* McGraw-Hill, London.
10. Carslaw, H.S.; and Jaeger, J.C. (1959). *Conduction of heat in solids*. Second Ed., Oxford University Press, Oxford,
11. Harmathy, T.Z. (1988). *The SFPE handbook of fire protection engineering.* Society of Fire Protection Engineers / National Fire Protection Association, Boston.

12. Yuan, J. (2009). *Fire protection performance of intumescent coating under realistic fire conditions.* Ph.D. Thesis, School of Mechanical, Aerospace and Civil Engineering, University of Manchester.
13. Cabrera, J.G.; and Lynsdale, C.J. (1988). A new gas permeameter for measuring the permeability of mortar and concrete. *Magazine of Concrete Research*, 40(144), 177-182.
14. ASTM C 457 (2000). *Standard test method for microscopical determination of parameters of the air-void system in hardened concrete.* Annual Book of ASTM Standards, Vol. 4.02, American Society for Testing and Materials, West Conshohocken, Pennsylvania.